Conference paper

Maria Margarida Mateus, Sandro Matos, Dinis Guerreiro, Paulo Debiagi, Daniela Gaspar, Olga Ferreira, João Carlos Bordado and Rui Galhano dos Santos*

Liquefaction of almond husk for assessment as feedstock to obtain valuable bio-oils

https://doi.org/10.1515/pac-2019-0304

Abstract: Almond husk liquefaction can be envisaged as an alternative to fossil sources which are becoming exhausted. Lately, the polyols obtain from the lignocellulosic biomass have been under investigation for the production of sustainable chemicals, fuel, materials or other commodities. Within this context, acid-catalyzed liquefaction of such lignocellulosic biomass has been successfully used to access highly functionalized compounds that can be used to replace those produced from petroleum. Almond shells waste can be considered to be part of the lignocellulosic biomass. Its main constituents of are cellulose, hemicellulose, and lignin. In this assay, the biochemical composition of almond husk was estimated based on atomic mass balances, and at the same time, the pyrolysis outcome was also estimated using a kinetic model using some reference compounds. In order to evaluate the use of almond waste as a substrate for acid-catalyzed liquefaction, the most favorable conditions of the liquefaction process were investigated. To better understand the liquefaction process, response surface methodology, in particular, central composite face-centered factorial design was used to set an array of 17 experiments including three replications at the center point leading to the development of a reaction model for further prediction and optimization of the liquefaction outcome. The effect of temperature (120–150 °C), time (20–200 min) and catalyst amount (0.5–5 wt. %) was investigated and a predictive model established.

Keywords: almond shell; ICS-29; liquefaction; pyrolysis; RSM; simulation; TGA.

Introduction

Over the last decades and with the increased demand for oil-derived products allied with its foreseen depletion, alternatives to such source of raw materials has been investigated and sought. That envisaged alternative should be competitive with the fossil sources regarding products quality and at the same time with sustainable costs. So, to cope the need and reliance on products derived from oil, the alternative sources should cause much less adverse repercussions on the environment while being, at the same time, economical and environmentally sustainable. Within this context, many resources have been the allocated to the research of the use of lignocellulosic biomass, as an alternative to fossil sources, due to its availability and

Article note: A collection of invited papers based on presentations at the 29th International Carbohydrate Symposium (ICS-29), held in the University of Lisbon, Portugal, 14–19 July 2018.

***Corresponding author: Rui Galhano dos Santos,** CERENA-Centre for Natural Resources and the Environment, Instituto Superior Técnico, Av. Rovisco Pais, 1049-001 Lisboa, Portugal, e-mail: rui.galhano@tecnico.ulisboa.pt
Maria Margarida Mateus: CERENA-Centre for Natural Resources and the Environment, Instituto Superior Técnico, Av. Rovisco Pais, 1049-001 Lisboa, Portugal; and Engineering Department, Universidade Atlântica, Fábrica da Pólvora de Barcarena, 2730-036 Barcarena, Oeiras, Portugal
Sandro Matos, **Dinis Guerreiro**, **Daniela Gaspar**, **Olga Ferreira and João Carlos Bordado:** CERENA-Centre for Natural Resources and the Environment, Instituto Superior Técnico, Av. Rovisco Pais, 1049-001 Lisboa, Portugal
Paulo Debiagi: Dipartimento di Chimica Materiali ed Ingegneria Chimica "Giulio Natta", Politecnico di Milano, Piazza Leonardo da Vinci 32, Milan, Italy

low cost. The availability of biomass derived from the industrial or feeding sector as wastes can be faced as a source of chemicals platform. Such platform may be useful to mitigate the environmental impact of the goods and commodities presently manufactured.

The annual production of almond, the seed of a tree, *Prunus dulcis*, syn. *Prunus amygdalus*, a tree that is widespread throughout the world, has doubled in the last decade, reaching a sum of ca. three million tonnes globally [1]. The residues of such industry reach 35–75 % of the total fruit weight [2]. Due to the lack of commercial or industrial interest, these residues are typically incinerated or just discarded, causing environmental impact. Air pollution, soil erosion and decreases soil biological activity are some of such issues. Moreover, exploiting those by-products residues may also represent a farmer's secondary earnings from plantation [3]. Almond husk has already been used as a bio-waste resource in wood-based composites [3, 4], as adsorbents of dyes [5] or metals [6], activated carbons [7], bio-methane production [8] or in studies regarding gasification [9].

The biochemical composition of almond shell depends on its variety as well as on its harvest location. Although generally, is composed mainly of cellulose, lignin, hemicellulose along with some extractives [10]. Much of the extractives found in the plant kingdom, i.e. flavonoid derivatives [11], are very interesting due to their anti-oxidant capacity, thus they can stabilize the products derived from the biomass that contain them. Almond wastes are an abundant, inexpensive and readily accessible source of raw material [12].

Lately, the liquefaction of biomass either via pyrolysis [13, 14] or direct liquefaction [15], although not being an entirely modern concept, has been widely studied and reviewed [16] due to the increasing interest of scientific community on those processes. The liquefaction involving alcohols as solvents has become a central process for many scientists, who are aiming the production of bio-oils from lignocellulosic biomass [17–19].

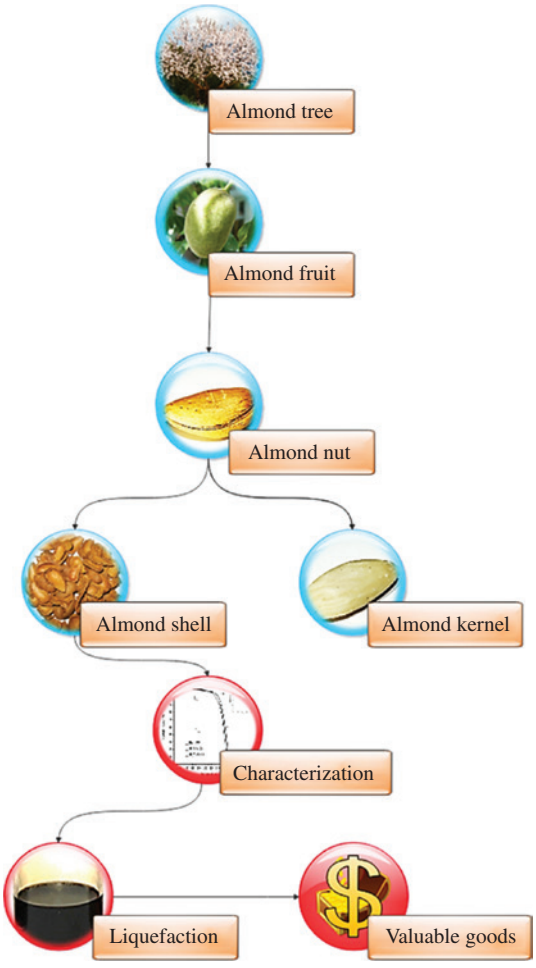

Fig. 1: Methodology envisaged for the valorisation of almond waste.

The liquefaction products, consisting of a mixture of compounds can be upgraded [16] and used in a biorefinery, producing added value compounds in the alternative to those that result from oil fractioning. For instance, the refined products can be used afterward as fuels [20–22], polyols for foam [23–25], adhesives [26, 27], the chemical building blocks among others [28–30].

The optimization step is critical in the improvement of the performance of the process, allowing, therefore, the development of an efficient methodology under investigation. Different types of methods are used to design reduced experiments arrays, and its further statistical interpretation has been exploited for the optimization of chemical processes. One of the methods, often used, is the response surface methodology (RSM). The relationships between dependent and independent variables and its impact on one or more responses to those variables are explored leading to the development of the mentioned mathematical model. With this method, fewer experiments are needed in opposite to the conventional optimization approach based on trial by error would usually require [31, 32].

To the best of our knowledge, the liquefaction process of almond waste was never previously reported. The purpose of this paper is to present a study carried for the thermochemical liquefaction of almond wastes catalyzed by p-toluenesulfonic acid and its further optimization using RSM. Computational simulation methods were used to estimate the approximate determination of such composition as well as to simulate the pyrolysis process of almond husk [33, 34]. The simulation of the pyrolysis process is essential for the validation of the biochemical composition estimation and to compare the yield of the liquid fraction of the pyrolysis process with that obtained from direct liquefaction. The result of this work will be very useful to implement a methodology to valorize this by-product which has almost no market value, regardless of the existence of studies demonstrating the suitability of this biomass for the production of activated carbons or on the conversion of this biomass into bio via pyrolysis. Still there are none on the liquefaction with polyhydric alcohols (Fig. 1).

Materials and methods

Materials and chemicals

Almond shells were provided by local producers. They were used without being subjected to any pre-treatment. The reagents used were chemical grade. 2-ethyl-hexanol, diethylene glycol, p-toluenesulfonic acid, tetrahydrofuran, methanol, acetone, potassium hydroxide (0.5 M and 0.1 M in ethanol, titration solutions) used were chemical grade (Sigma-Aldrich).

Liquefaction procedure

The experimental procedure adopted was as described by Mateus et al. [35]. A reactor containing p-toluene sulfonic acid and 10 % w/w of biomass based on its dry weight in a mixture of 1:2 (w/w) of 2-ethylhexanol and diethylene glycol was stirred at different temperatures ranging from 100 to 180 °C; for 20, 110 and 200 min and catalyst (p-toluenesulfonic acid) concentration from 0.5 to 5 wt. %. The combination of these factors is described in Section "Optimization of almond shell liquefaction". Afterward, the reaction is allowed to cool to room temperature.

Measurement of liquefaction extent

The residue was retrieved from the reaction crude by vacuum filtration. Afterward, the remaining insoluble products were washed with methanol and acetone.

After drying the residues, the conversion ratios were calculated by eq. 1:

$$\text{Conversion yield } (\%) = 1 - \left(\frac{M_r}{M_i}\right) \times 100 \tag{1}$$

where M_r is the mass of the final dried solid residue and M_i is the mass of the biomass used in the liquefaction process [36].

Chemical and calorific analysis

The elemental composition concerning carbon, hydrogen, and nitrogen of the various samples were obtained via elemental analysis using a LECO TruSpec CHN analyzer instrument. While for sulfur, the determination was carried out in a LECO CNS2000. The oxygen content was estimated by the difference between 100 % and the sum of carbon, hydrogen, sulfur and nitrogen fractions. The calorific values were determined with a calorimeter LECO AC500.

ATR experiments

ATR experiments were crucial to demonstrate the presence of carbohydrate and phenolic derivatives within the bio-oil obtained by liquefaction of almond shell proving, thus, the liquefaction process occurred. The FTIR-ATR spectra were obtained using an ATR accessory. Spectra were recorded on a Thermo Nicolet Nexus instrument (128 scans with a resolution of 4 cm^{-1}).

Thermal gravimetric analysis (TGA)

Thermogravimetric experiments were carried out in a differential thermogravimetric analyzer (STA449F5/ Netzsch). The precision of the temperature measurement was ±2 K. For each sample, 12 mg of biomass was heated from 30 °C up to 590 °C under dynamic conditions at a heating rate of 10 K/min on aluminum oxide crucible. The TGA experiments were carried out at atmospheric pressure, and the equipment was purged with a nitrogen flow of 20 mlN min^{-1}. This experiment was useful for validating the model used for the determination of the biochemical composition as well as for simulating the pyrolysis products.

Calculations

Determination of approximate biochemical composition and pyrolysis simulation via computational tools

CRECK (Chemical Reaction Engineering and Chemical Kinetics) modeling group develops kinetic models for biomass pyrolysis. The mathematical models are entirely predictive and are able to describe the thermal decomposition of a large amount of lignocellulosic biomasses in a broad range of conditions, with reliable results. In this case, we applied the characterization procedure reported by Debiagi et al. [33] and the updated kinetic model proposed by the same authors [34] to compare with the experimental data obtained. The model relies on strong simplifications to describe this multicomponent, multiphase and multiscale problem. A few reference species are considered to represent the main components of the biomass. CELL and HECELL are the reference species for the polysaccharides cellulose and hemicellulose. LIGO, LIGH, and LIGC are lumped compounds representing lignin fragments, rich in oxygen, hydrogen, and carbon, respectively. TANN and TGL are lumped species representing hydrophilic and hydrophobic extractives present in biomass. Each reference species follows its degradation path described with multistep first-order kinetics outlined in the Arrhenius form. The kinetic parameters, together with the stoichiometries are reported elsewhere [34]. Also, the model is able to predict quantitatively the expected pyrolysis products, which stabilize in three phases at room temperature: a solid char, a liquid bio-oil, and a permanent gas. The applied kinetic model does not consider the effect of catalysts. In this sense, the simulation reports the expected products for a non-catalyzed

process. These yields obtained with simulations are useful to support and compare with the catalytically-aided process, investigating whereas significant differences are present.

RSM experiment design and statistical analysis

The design of experiments (DoE) technique, namely response surface methodology (RSM) was used to optimize the liquefaction process of almonds husk. The optimization of the process was accomplished by monitoring the effect/interaction of three independent variables (factors), namely temperature (°C), reaction time (minutes) and the amount of the catalyst (w/w %) on the liquefaction yield (response). A central composite face-centered (CCF) factorial design (Fig. 2) comprising one experiment for each cube's vertices (factorial points), face-centered (axial points), and three replicates of the cube's central point (0,0,0) corresponding to 17 experimental points according to Table 1, was used for that purpose. The three-factor considered were temperature, reaction time and the amount of the catalyst ranged from 100 to 180 °C, 20–200 min and 0.5 %–5 % w/w, respectively. MODDE software (Umetrics AB, Sweden) was used to set up the experimental design and evaluate the partial least squares (PLS) model.

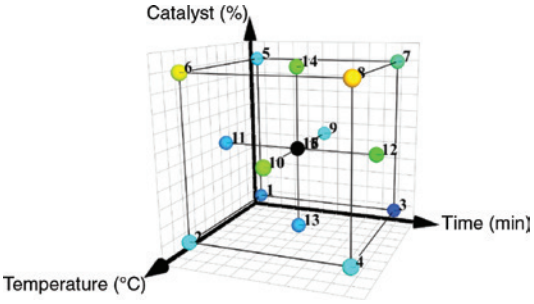

Fig. 2: Central composite face center designs for the optimization of almond wastes liquefaction considering three independent variables.

Table 1: Layout of the matrix of experiments and responses, codes of the independent variables for the design of experiment.

Exp. no.	Exp. name	Run order	Coded value		
			x_1	x_2	x_3
1	N1	16	−1	−1	−1
2	N2	15	1	−1	−1
3	N3	1	−1	1	−1
4	N4	13	1	1	−1
5	N5	4	−1	−1	1
6	N6	9	1	−1	1
7	N7	3	−1	1	1
8	N8	11	1	1	1
9	N9	10	−1	0	0
10	N10	2	1	0	0
11	N11	12	0	−1	0
12	N12	17	0	1	0
13	N13	8	0	0	−1
14	N14	5	0	0	1
15	N15	14	0	0	0
16	N16	6	0	0	0
17	N17	7	0	0	0

The multiple linear regression (MLR) procedures (Modde software) was used to fit data acquired after the completing the trials defined within the experimental design. As a starting point the following second-order polynomial equation two was used to build a model to describe and predict the outcome responses to the factors variations:

$$Y = \beta_0 + \sum_{i=1}^{3} \beta_i x_i + \sum_{i=1}^{3} \beta_{ii} x_i^2 + \sum_{i=1}^{2} \sum_{j=i+1}^{3} \beta_{ij} x_i x_j \quad (2)$$

where Y is representing the response (yield, %); x_i and x_j the encoded independent variables and β_0, β_i, β_{ii}, and β_{ij} the intercept, linear, quadratic, and interaction coefficients, respectively. Contour plots were plotted using the fitted quadratic polynomial equation obtained from the better regression analysis, changing two of the independent variables and holding the remaining one independent variable fixed.

The MODDE software package provides the necessary tools to calculate the fraction of variation of the response that can be explained by the model (R^2) as well as those predicted by the model (Q^2). Both statistical indicators should be one for a perfect model, which is usually not attainable, so values higher than 0.99 allows to build a strong, robust and reliable model.

Statistical significance was evaluated using the Analysis of Variance (ANOVA) considering as a base the *p*-value less than 0.05 significant (confidence level of 95 %). The predictability of the developed model was confirmed, validated by conducting an experiment using a combination of the three independent variables. The combination considered was not part of the original experimental design but within the limits of the values considered for the experimental design [31, 37, 38].

Results and discussion

Biochemical and pyrolysis simulation

An initial characterization of almond husk concerning its biochemical composition was estimated following the method proposed by Debiagi et al. [33, 34]. This evaluation was conducted using *in silico* tools, in order to avoid the use of experiments that most of the times are quite expensive and very time consuming. This procedure only requires the elemental composition of the sample together with moisture and ash contents. Table 2 shows the almond shell elemental composition obtained experimentally. The CxH plot in Fig. 3 illustrates the composition of reference components used to characterize the biomass. In order to obtain a feasible composition, the sample must fall within the characterization limits, obtaining a linear combination of the components that can respect the atomic mass balances. Table 3 shows the biochemical composition obtained through the characterization model. The compounds present in Table 3 are the reference molecules that represent the main biochemical components of biomass. The meaning of these values is that almond shell is composed of 33.71 % of Cellulose, 27.47 % of Hemicelluloses, 36.75 of Lignin (sum of LIGO, LIGH, and LIGC), 7.69 % of Extractives (sum of TANN and TGL), 2 % of moisture and 5.7 % of ashes.

In order to validate the computed almond husk biochemical profile, the composition obtained from the characterization model was used as input for describing a pyrolisis reactor feed. In this case, we simulated

Table 2: Almond shell – elemental composition.

Almond shell **Elemental composition (experimental wt. %)**			
C	**H**	**O**	**N**
49.70	5.77	43.41	1.12

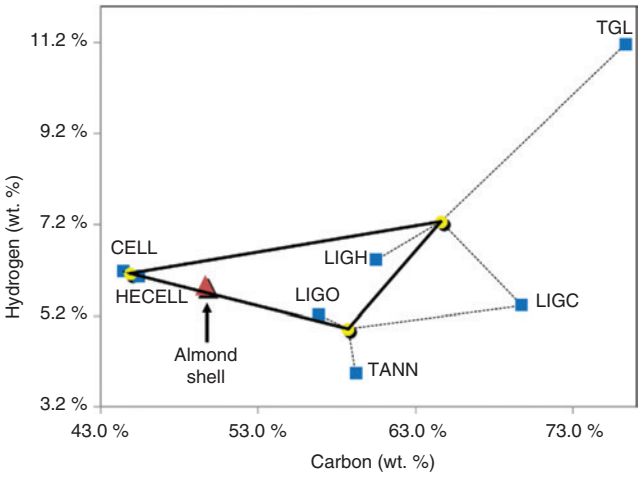

Fig. 3: CxH plot with the reference components (squares) and almond shell sample (triangle).

Table 3: Almond shell characterization – model predictions for biochemical composition.

Biochemical composition (characterization model wt. %)								
CELL	**HECELL**	**LIGO**	**LIGH**	**LIGC**	**TANN**	**TGL**	**Moist.**	**ASH**
33.71	27.47	18.84	14.81	3.10	7.27	0.42	2.00	5.7

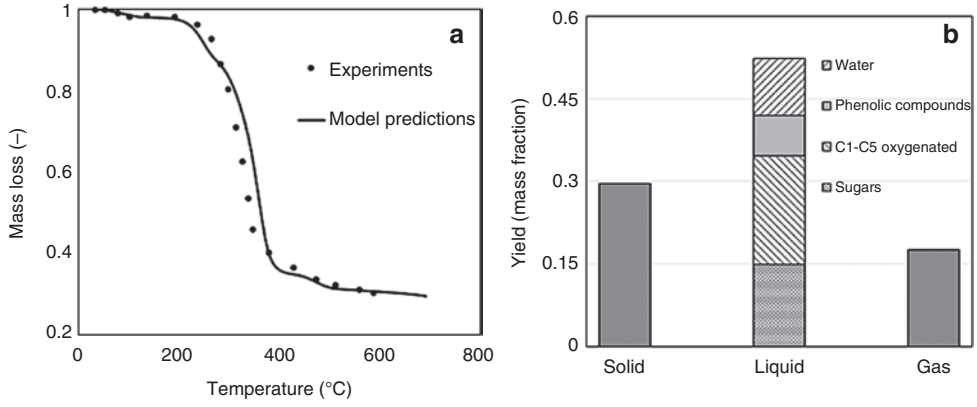

Fig. 4: Almond shell pyrolysis. (a) Experimental thermogravimetric analysis and model predictions. (b) Phase yields predictions of the pyrolysis products.

the thermogravimetric analysis as a perfect batch reactor at room temperature heated at a 10 K/min rate, at 1 bar. No heat and mass transfer and effect of catalysts are considered. Figure 4a compares the experimental mass loss under pyrolysis conditions for a sample of almond husk by thermogravimetric analysis (TGA) with that obtained by the developed model via simulation. A very similar behavior can be noted both on mass loss speed, temperatures, and final solid residue. The model is able to predict the pyrolysis behavior quite well, with minor discrepancies such as a slightly slower conversion at about 50 % of the mass loss and a faster conversion at 90 % of the mass loss, when compared to the experimental data. Nevertheless, these deviations can be a result of the strong simplifications, both on the number of species that represent the feedstock and the number of reactions that describe the pyrolysis. These model simplifications are necessary in order to keep the low computational cost of the model when simulating complex reactors that consider transport phenomena in different scales. A useful additional outcome data of this simulation is the obtained products. Figure 4b

shows the phase yields with the liquids divided into four different groups of compounds: sugars, oxygenated compounds containing from one to five carbon atoms, phenolic compounds, and water (moisture). The data obtained from simulation, are very useful to compare the fraction of the liquids that could be accessed either by pyrolysis or by liquefaction of biomass. Thus, the performance of the liquefaction process can be evaluated.

Optimization of almond shell liquefaction

The optimization of almond shell liquefaction was carried out using three experimental factors (temperature, time and catalyst amount) according to the experiments conducted and described in Table 4.

The higher liquefaction yield, ~82 %, was obtained when almond wastes were stirred for 200 min at 180 °C with 5 wt. % of p-toluene sulfonic acid. Despite the high value obtained for the conversion of biomass, it is necessary to draw attention that this was obtained within the limits of the experimental domain established for the study, and which are generally applied in the approach in question. Still, the value obtained, 82 %, is about 30 % higher than it could be, according to what was obtained by simulation obtained by pyrolysis (Fig. 4b). It is thus demonstrated that although the conversion value was achieved at the limit of the established parameters, the liquefaction process is more advantageous than the pyrolysis for obtaining biooils from almond shells.

Regarding the development of the mathematical model for the liquefaction process, Tilmatine et al. [39] suggested that it can be validated with the identification and detection of any mistaken response resulting from operational errors. Such values should be considered as outliers. Another condition is the evaluation of the predictive and experimental indicators which should be as close as possible to the unit. Additionally, a complementary experiment should be conducted with random levels of the factors under investigation, within the considered range of the experimental design. The outcome of such test should then be compared with the response predicted by the model to check its predictability.

The experimental data were analyzed with MODDE tools and then fitted with multiple linear regression (MLR). The obtained model, (Table 5, model #1) indicated that 93.8 % of the responses variation could be

Table 4: The layout matrix of the liquefaction experiments conducted with the correspondent experimental and predicted responses.

Exp. no.	Exp. name	Run order	Coded values			Real values			Response	
			x_1	x_2	x_3	Temp (°C)	Time (min)	Catalyst (w/w %)	Yield exp. (%)	Yield pred. (%)
1	N1	16	−1	−1	−1	100	20	0.5	12.33	9.16
2	N2	15	1	−1	−1	180	20	0.5	24.35	25.82
3	N3	1	−1	1	−1	100	200	0.5	6.63	7.33
4	N4	13	1	1	−1	180	200	0.5	26.40	23.99
5	N5	4	−1	−1	1	100	20	5	20.50	21.69
6	N6	9	1	−1	1	180	20	5	69.40	69.92
7	N7	3	−1	1	1	100	200	5	35.94	35.68
8	N8	11	1	1	1	180	200	5	81.95	83.91
9	N9	10	−1	0	0	100	110	2.75	25.31	23.52
10	N10	2	1	0	0	180	110	2.75	60.83	55.97
11	N11	12	0	−1	0	140	20	2.75	14.32[a]	–
12	N12	17	0	1	0	140	200	2.75	52.59[a]	–
13	N13	8	0	0	−1	140	110	0.5	14.80	21.63
14	N14	5	0	0	1	140	110	5	57.85	57.86
15	N15	14	0	0	0	140	110	2.75	37.72	39.74
16	N16	6	0	0	0	140	110	2.75	41.76	39.74
17	N17	7	0	0	0	140	110	2.75	39.97	39.74

[a]Considered to be outliers, a more robust model was achieved upon their discarding.

Table 5: Linear, quadratic and interaction coefficients and its significance to the developed model.

	Model# 1				Model# 2				Adopted model			
	Coeff. SC	Std. Err.	*p*-Value	Conf. int(±)	Coeff. SC	Std. Err.	*p*-Value	Conf. int(±)	Coeff. SC	Std. Err.	*p*-Value	Conf. int(±)
Constant	39.4779	3.5149	0.0000	8.3116	39.8014	1.9541	0.0000	5.0233	39.7430	1.3739	0.0000[a]	3.1683
temp	16.2231	2.5976	0.0004	6.1424	16.2231	1.0703	0.0000	2.7513	16.2231	1.1495	0.0000[a]	2.6508
Time	6.2610	2.5976	0.0467	6.1424	3.0425	1.1966	0.0517	3.0761	3.0425	1.2852	0.0454[b]	2.9637
Cat	18.1128	2.5976	0.0002	6.1424	18.1128	1.0703	0.0000	2.7513	18.1128	1.1495	0.0000[a]	2.6085
temp*temp	3.8351	5.0184	0.4697	11.866	3.2689	3.0897	0.3384	7.9425	–	–	–	–
Time*Time	−5.7800	5.0184	0.2872	11.866	−4.9107	4.0874	0.2833	10.507	−5.0568	1.8813	0.0275[b]	4.3384
Cat*Cat	−2.9074	5.0184	0.5805	11.866	−3.4735	3.0897	0.3119	7.9425	–	–	–	–
temp*Time	0.6078	2.9042	0.8401	6.8675	0.6078	1.1966	0.6331	3.0761	–	–	–	–
temp*Cat	7.8915	2.9042	0.0298	6.8675	7.8915	1.1966	0.0012	3.0761	7.8915	1.2852	0.0002[a]	2.9637
Time*Cat	3.9561	2.9042	0.2153	6.8675	3.9561	1.1966	0.0213	3.0761	3.9561	1.2852	0.0151[b]	2.9637
	$Q^2=0.469$		Cond. no. = 4.438		$Q^2=0.870$		Cond. no. = 4.438		$Q^2=0.940$		Cond. no. = 2.704	
	$R^2=0.938$		RSD = 8.214		$R^2=0.992$		RSD = 3.385		$R^2=0.984$		RSD = 3.635	
	N = 17 DF = 7		R^2 adj. = 0.847		N = 15 DF = 5		R^2 adj. = 0.976		N = 15 DF = 8		R^2 adj. = 0.973	

[a]Confidence level 99.9 %, [b]Confidence level 95 %, underlined were considered not significant.

explained by the model ($R^2=0.938$), which thereby cannot be viewed as a weak model. Although the predictive ability of the model was quite low, only 46.9 % of the reaction outcome could be predicted ($Q^2=0.469$), and there were some coefficients considered by the model that was not significant with high *p*-values at a confidence level of 95 % of ($p>0.05$). A better analysis of the experimental data with MODDE tools package identified the presence of outliers (reactions N11 and N12) which were then rejected. A new model was so obtained (Table 5, model #2). The new predictive equation has now presented an excellent correlation regarding the explanation of the collected data ($R^2=0.992$) and good ability to generalize the model to new and unseen results with a predictability of 87 % ($Q^2=0.870$). Usually considered that R^2 and Q^2, the first two columns in Fig. 5a, should be close in value and their difference should not be more than 20 % [40], in this particular case is ~14 %. Other interpretations of the relationship between these two indicators refer that the difference between both should not be higher by more than 0.2–0.3 ($R^2-Q^2=0.12$). Thus since there was no such difference, the obtained model can be considered as an appropriate one, but not yet an excellent model.

The predictive power indicated by $Q^2>0.5$ is regarded as a good model, but a $Q^2>0.9$ is aimed since for such values the model could be considered as excellent [37]. Thus, this model could be refined and improved. The confidence level of the experimental design was fixed at 95 %; the *p*-value determines the impact of each

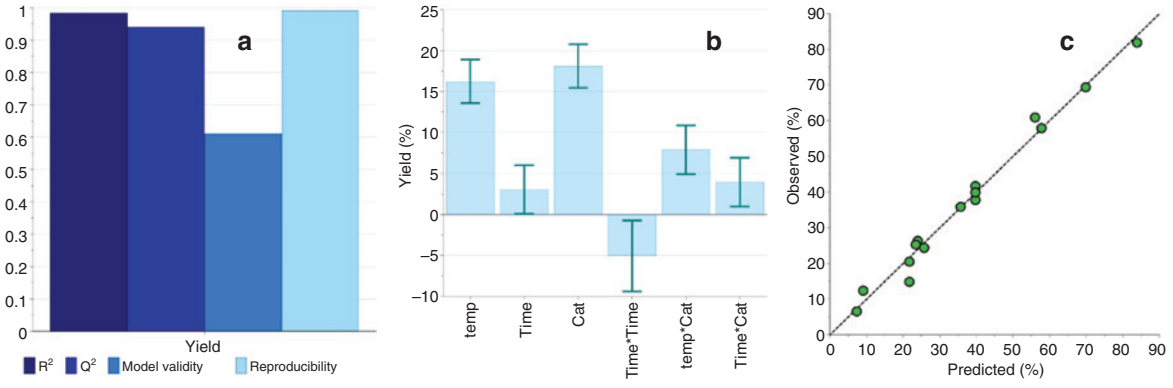

Fig. 5: (a) Graphical summary of the statistical key parameters ($R^2=0.98$, $Q^2=0.94$, model validity = 0.61, and reproducibility = 0.92), (b) graphic of the coefficients contribution to the model of the almond liquefaction response, (c) plot of the correlation of the observed vs. predicted values of almond wastes liquefaction.

term (factor) in the model mathematical expression. Non-significant terms have a *p*-value higher than 0.05. Therefore, the terms of the model #2, temp*temp, Cat*Cat, and temp*Time were disregarded from the model due to their high *p*-values. The remaining terms lead to a model where all the terms were statistically significant ($p > 0.05$). The evaluation of the coefficient plot of the model (Fig. 5b) indicates the contribution of each term and how they affect the reaction outcome. Moreover, the significance of each term (factor) in the model is determined by the size of the coefficients (bars) and their error bars. All terms are now significant since there is none which encompasses an error bar spanning zero ($p > 0.05$) being such condition observed only in non-significative terms. The summary of the fit plot for the obtained model validates the statistical accuracy of the model (Fig. 5a). The model validity is 0.61, values larger than 0.25 the model are considered to be in the same range as the pure error. On the other hands, the reproducibility of the model (variation amongst the center point runs) was 0.99. A reproducibility of 1 indicates that the pure error is null. Overall the values presented in Table 5, and on the graph plotted in Fig. 5a, and b showed a good and robust model. Therefore, the model can be represented by the eq. 3:

$$Y\,(\%) = 39.74301 + 16.22312T + 3.04250t + 18.11282C - 5.05684t^2 + 7.89153TC + 3.95610tC \quad (3)$$

where Y is the liquefaction yield (%), T is the temperature; t is the time and C is the amount of catalyst.

Table 5, presents all the main effects and given interactions that are significant for the experiment response. The catalyst amount proved to be the factor with more effect on the residue content, followed by temperature, temperature/catalyst amount, time/catalyst amount interaction, time, and at last the square time interaction has an adverse impact on the model.

The demonstration of the predictive ability of the model can be judged by plotting the predicted versus experimental values of the liquefaction yield. The fit to the line of parity exhibited a high coefficient of determination ($R^2 = 0.985$) indicating that the model can forecast the liquefaction outcome with high reliability (Fig. 5c) [40].

The analysis of variance (ANOVA) (Table 6), shows that the regression and the lack-of-fit has a *p*-value less than 0.001 and higher than 0.05, respectively, demonstrating once again the reliability of the model.

This model permitted to obtain optimal response surfaces (Fig. 6) and contour plots (Fig. 7) for the liquefaction yield response to the variations of the parameters considered for this study. The contour plot provided the 2-dimensional view of the surface, connecting the zones with the same response to the change of the considered factors to produce contour lines. These charts are very useful for predicting the liquefaction outcome relatively to the reactional conditions considered or available. On the other hand, the 3D surface plot displays a 3-dimensional view of the surface response. Like contour plots, 3D surface plots are useful for establishing response values and operating conditions. Although, these plots provide a more accurate visualization of how the considered factors affect the response surface since the profile of the reaction can be observed.

The statistical results depicted in Fig. 6, as well as Fig. 7, revealed that the suitable liquefaction conditions to maximize the conversion is achieved when the almond waste is stirred for 200 min with 5 w/w % of the catalyst at 180 °C the higher yield was obtained ~80 %.

Table 6: Analysis of Variance of the developed model by design of experiment.

Yield	DF	SS	MS (variance)	F	*p*-Value	SD
Total	15	27 307.4	1826.49			
Constant	1	20 596.1	20 586.1			
Total corrected	14	6811.29	486.521			22.0572
Regression	6	6705.27	1117.6	84.573	0.000	33.4305
Residual	8	105.716	13.2146			3.63518
Lack of Fit (Model error)	6	97.6702	16.2784	4.04618	0.211	4.03518
Pure error (Replicate error)	2	8.04629	4.02314			2.00578

DF, Degrees of freedom; SS, sum of squares; MS, mean square; SD, standard deviation.

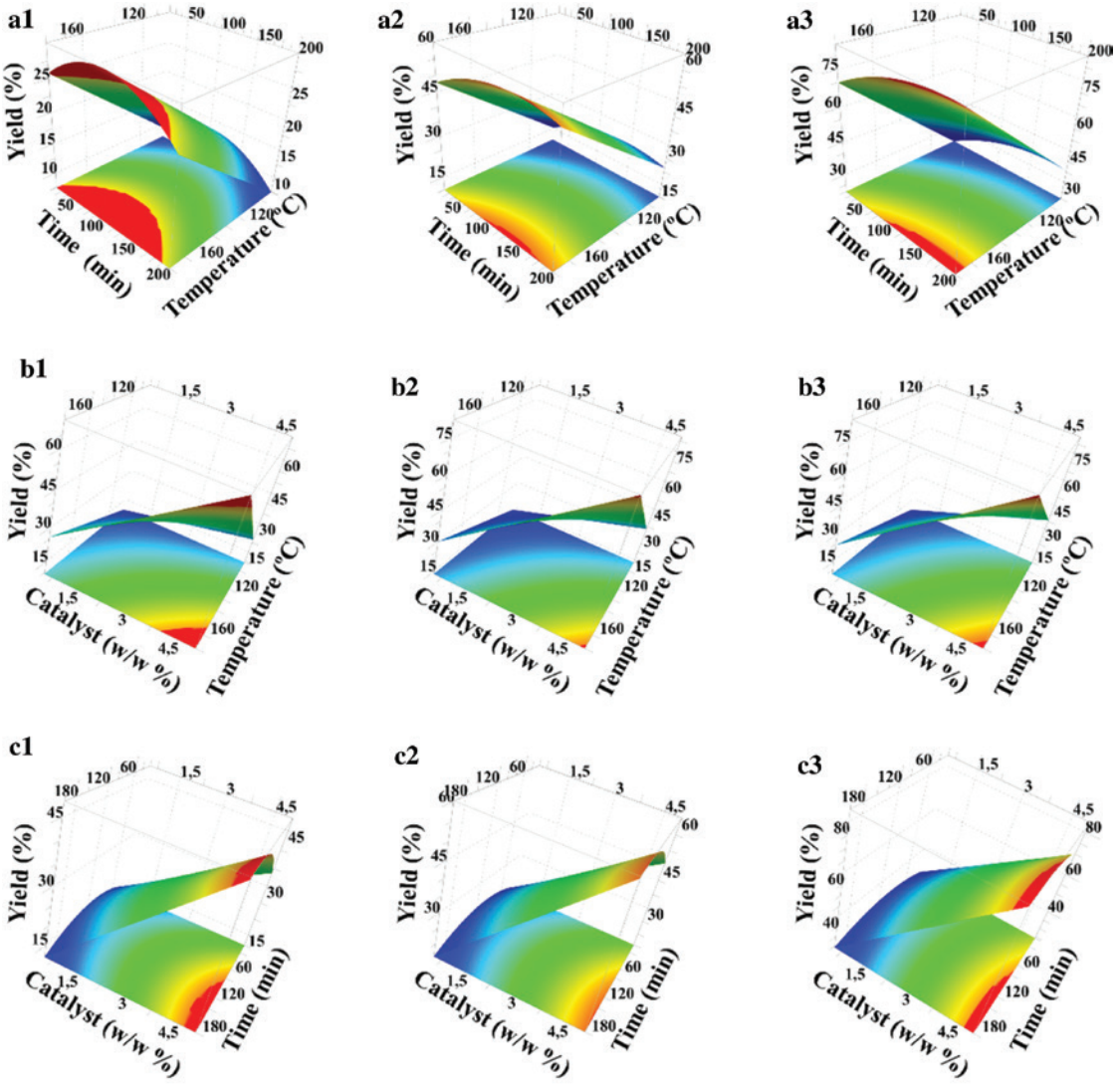

Fig. 6: The surface contour plots concerning the response (yield, %) to (a) time (min) vs. temperature (°C) (**a1**. 0.5, **a2**. 2.75 and **a3**. 5 w/w % of catalyst); (b) catalyst (w/w %) vs. temperature (°C) (**b1**. 20, **b2**. 110 and **b3**. 200 min)and (c) catalyst (w/w %) vs. time (min) (**c1**. 100, **c2**. 140 and **c3**. 200 °C) of almond wastes liquefaction.

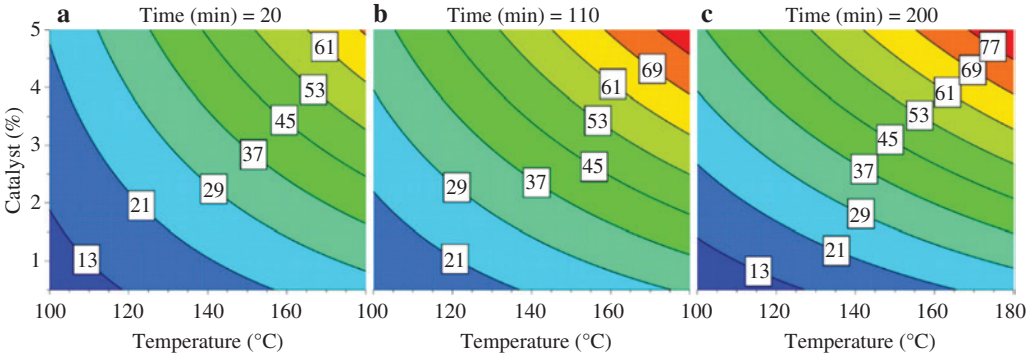

Fig. 7: The contour plots concerning the response (yield, %) to the variation of catalyst (w/w %) vs. temperature (°C) after (a) 20 min, (b) 110 min and (c) 200 min of the almond wastes liquefaction.

Table 7: Validation of the model using combinations of independent variables, which were not part of the original experimental design but were within the established limits.

	Temperature (°C)	Time (min)	Catalyst (w/w %)	Yield (%)
Predicted	150	120	2	33.88–40.57
Experimental				34.40

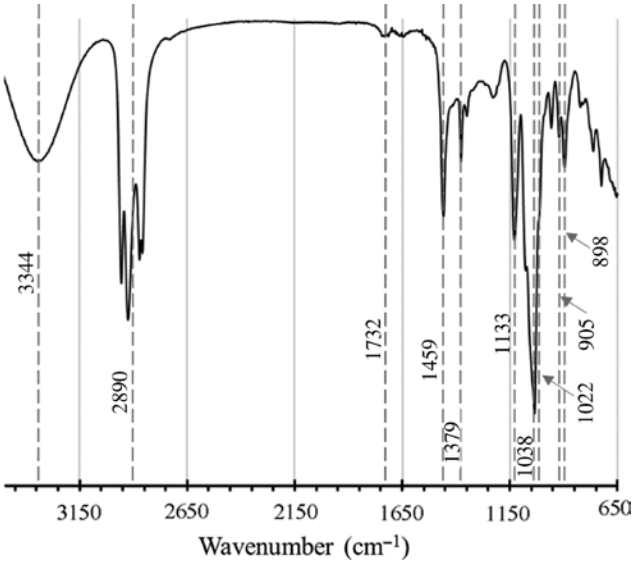

Fig. 8: ATR-FTIR spectra from liquefied almond waste.

In order to validate the predictive quality of the developed model, we conducted an additional experiment with random values of temperature, time and catalyst amount. Afterward, we compared the response obtained with that predicted by the mathematical model. The result is given in Table 7. The experiment outcome falls between the predicted response limits, validating the good predictive quality of the mathematical model obtained using RSM. We can, therefore, conclude that the model expressed by the mathematical eq. 3 is a reliable fitting quite well the experimental data as well as predicting the liquefactions outcome.

Bio-oil characterization by ATR-FTIR

The infra-red spectroscopy of the liquefied almond waste was accessed via ATR-FTIR at room temperature. The resulting spectra are exhibited in Fig. 8. The spectra present a broad peak at 3344 cm^{-1}, which is typical of OH groups. The presence of those hydroxyl groups can overcome either from the depolymerization of cellulose/hemicellulose and/or other alcoholic moieties/residues. The signal at 2890 cm^{-1} corresponds to C–H stretching, widely spread in the structures existent on the liquefied mixture. The weak peak at 1732 cm^{-1} may be the result of the carbonyl stretching in unconjugated ketone, ester or carboxylic groups [41–43]. The presence of this signal on the liquefied products spectra indicates that the raw material was liquefied. Such signal that may correspond to the carbonyl resulting from the decomposition of cellulose and related compounds. The intense band at 1038 cm^{-1} is the consequence of the aromatic C–H in-plane deformation for guaiacyl type material found in lignin [44]. Also, the spectra display the characteristic bands of benzene rings (1459 cm^{-1}) and syringyl rings (1379 cm^{-1}), corroborating that the depolymerized products contain, in fact, derivatives from lignin. On the other hand, focusing on a particular spectral zone, corresponding to the anomeric linkages (950–750 cm^{-1}) [45, 46], the small band found at 905 cm^{-1}, typical of β-anomers, denotes the presence

of β-glycosidic linkages between sugar units. Another signal also characteristic of carbohydrates scaffold corresponding to the asymmetric out-of-phase ring stretching which causes a C–H equatorial deformation vibration band in the α- and β-pyranoses appears at 898 cm^{-1}. An additional peak (1133 cm^{-1}) observed in the spectra of most carbohydrates, attributed mainly to the stretching vibrations of C–O–C bonds of the heterocyclic backbone is also visible in this spectra. Cellulose, hemicellulose derivatives, and di- and polysaccharides with 1→4 glycosidic linkage are some of those structures. Finally, a particular signal corresponding to the glucose C–O or C–H bending vibration is slightly visible at 1022 cm^{-1} [26, 47]. Hence, the liquefied product is highly functionalized. Future studies will be focused on the identification of the major mixture components.

Conclusions

First and foremost, the acid-catalyzed liquefaction of almond shell that, to the best of our knowledge, was not yet described was accomplished. The bio-characterization of biomass was obtained by simulation using data from elemental analysis and TGA experiments. The obtained data permitted to estimate and predict towards computational tools its biochemical composition.

The DoE method allowed to develop a mathematical model to forecast the almond waste acid-catalyzed liquefaction outcome using RSM within the parameters considered for this study. The obtained model, eq. 3, can be considered quite good and robust according to the statistical analysis conducted. The disclosed approach demonstrated that the liquefaction process could convert more than 77 % of biomass into a liquid fraction. In contrast, the pyrolysis process affords no more than ≈ 50 % of liquids. Thus the liquefaction of almond husks in polyhydric alcohols is a good approach for those who intend to obtained liquid fractions for further use.

This study turns out to be significant because, in an era where the concept of biorefinery begins to cease to be a mirage to become a tangible reality, it is very important to find biomasses that can be processed to produce sustainable products. In addition, wastes from transformative activities that are often simply burned, and thus losing all the value that could be withdrawn, can become a source of income for those who produce them. The study of the characteristics of the bio-oleo could be further deepened but at this point the main purpose and objective was to make sure that the liquefaction of this residue was actually possible. In the future it is our will to deepen the knowledge about the bio obtained, knowing beforehand, that bio-oils obtained from analogs sources have been successfully tested in the production of adhesives [48], foams [49–51] and with energetic potential [52, 53]. This study can also be used as a tool for the scale-up of the process to industrial scale.

Acknowledgment: The authors gratefully acknowledge the support of the CERENA (Funder Id: http://dx.doi.org/10.13039/501100001871, strategic project FCT-UID/ECI/04028/2019) funded by Fundação para Ciência e a Tecnologia, Portugal. Paulo Debiagi gratefully acknowledges the financial support from CAPES Foundation, Ministry of Education of Brazil-Science without Borders Mobility Program – Full Ph.D. Scholarship. The CRECK modeling group from the Milan Polytechnic Institute, and in particular Prof. Tiziano Faravelli, are also recognized for their collaboration.

References

[1] Statistics division. Crops Production http://faostat3.fao.org/browse/Q/QC/E (Accessed date Nov 9, 2016).
[2] A. Ebringerová, Z. Hromádková, Z. Košťálová, V. Sasinková. *BioResources* **3**, 60 (2008).
[3] H. Pirayesh, A. Khazaeian. *Compos. B Eng.* **43**, 1475 (2012).
[4] L. Quiles-Carrillo, N. Montanes, D. Garcia-Garcia, A. Carbonell-Verdu, R. Balart, S. Torres-Giner. *Compos. B Eng.* **147**, 76 (2018).
[5] M. Jabli, E. Gamha, N. Sebeia, M. Hamdaoui. *J. Mol. Liq.* **240**, 35 (2017).

[6] N. Maaloul, P. Oulego, M. Rendueles, A. Ghorbal, M. Díaz. *J. Environ. Chem. Eng.* **5**, 2944 (2017).
[7] J. M. V. Nabais, C. E. C. Laginhas, P. J. M. Carrott, M. M. L. Ribeiro Carrott. *Fuel Process. Technol.* **92**, 234 (2011).
[8] S. Ali, T. A. Shah, A. Afzal, R. Tabassum. *Energy Environ.* **29**, 742 (2018).
[9] N. Cerone, F. Zimbardi. *Energies* **11**, 1280 (2018).
[10] D. Nabarlatz, X. Farriol, D. Montané. *Ind. Eng. Chem. Res.* **44**, 7746 (2005).
[11] A. P. Rauter, R. G. Lopes, A. Martins. *Nat. Prod. Commun.* **2**, 1175 (2007).
[12] S. Hashemian. *Oriental J. Chem.* **30**, 2091 (2014).
[13] S. Thangalazhy-Gopakumar, W. M. A. Al-Nadheri, D. Jegarajan, J. N. Sahu, N. M. Mubarak, S. Nizamuddin. *Bioresour. Technol.* **178**, 65 (2015).
[14] M. T. H. Siddiqui, S. Nizamuddin, H. A. Baloch, N. M. Mubarak, M. M. Tunio, S. Riaz, K. Shirin, Z. Ahmed, M. Hussain. *Biomass Convers. Biorefin.* **8**, 857 (2018).
[15] R. Galhano dos Santos, P. Ventura, J. C. Bordado, M. M. Mateus. *Environ. Chem. Lett.* **15**, 453 (2017).
[16] H. A. Baloch, S. Nizamuddin, M. T. H. Siddiqui, S. Riaz, A. S. Jatoi, D. K. Dumbre, N. M. Mubarak, M. P. Srinivasan, G. J. Griffin. *J. Environ. Chem. Eng.* **6**, 5101 (2018).
[17] S. Nizamuddin, H. A. Baloch, N. M. Mubarak, S. Riaz, M. T. H. Siddiqui, P. Takkalkar, M. M. Tunio, S. Mazari, A. W. Bhutto. *Waste Biomass Valorization* 1 (2018). doi:10.1007/s12649-018-0206-0.
[18] M. Castellví Barnés, J. Oltvoort, S. R. A. Kersten, J. P. Lange. *Ind. Eng. Chem. Res.* **56**, 635 (2017).
[19] C. M. Patel, A. A. Barot, V. Kumar Sinha. *J. Appl. Polym. Sci.* **133**, (2016).
[20] F. W. Lichtenthaler. In *Fuels, Specialty Chemicals and Biobased Products from Agroindustrial Waste and Surplus*, F. Fava, P. Canepa (Eds.), pp. 230–253, Venezia (2008).
[21] R. Galhano dos Santos, J. C. Bordado, M. M. Mateus. *J. Clean. Prod.* **137**, 195 (2016).
[22] M. M. Mateus, J. C. Bordado, R. G. Dos Santos. *Fuel* **174**, 114 (2016).
[23] N. V. Gama, B. Soares, C. S. R. Freire, R. Silva, C. P. Neto, A. Barros-Timmons, A. Ferreira. *Mater. Des.* **76**, 77 (2015).
[24] M. H. Alma, M. A. Basturk, M. Digrak. *J. Mater. Sci. Lett.* **22**, 1225 (2003).
[25] Y. Yan, H. Pang, X. Yang, R. Zhang, B. Liao. *J. Appl. Polym. Sci.* **110**, 1099 (2008).
[26] R. G. dos Santos, R. Carvalho, E. R. Silva, J. C. Bordado, A. C. Cardoso, M. do Rosário Costa, M. M. Mateus. *Ind. Crops Prod.* **84**, 314 (2016).
[27] J. C. Bordado, E. Silva, R. Galhano Dos Santos, M. M. Mateus, A. C. Mesquita, M. D. R. Costa. WO2015034383 – Two-Component Natural Polymeric Water-Based Glues, Obtained From Derivatives Of Cork, 2015.
[28] A. M. C. Yona, F. Budija, B. Kričej, A. Kutnar, M. Pavlič, P. Pori, Č. Tavzes, M. Petrič, B. Kricej, A. Kutnar, M. Pavlic, P. Pori, C. Tavzes, M. Petric. *Ind. Crops Prod.* **54**, 296 (2014).
[29] J. Karger-Kocsis. *Express Polym. Lett.* **5**, 92 (2011).
[30] A. Ebringerová, T. Heinze. *Macromol. Rapid Commun.* **21**, 542 (2000).
[31] Y. Huang, H. Zheng, Y. Yan. *Appl. Biochem. Biotechnol.* **160**, 504 (2010).
[32] Q. L. P. Tan, X. N. T. Kieu, N. H. T. Kim, X. N. T. Hong. *Emir. J. Food Agric.* **24**, 25 (2012).
[33] P. E. A. Debiagi, C. Pecchi, G. Gentile, A. Frassoldati, A. Cuoci, T. Faravelli, E. Ranzi. *Energy Fuels* **29**, 6544 (2015).
[34] P. E. A. Debiagi, G. Gentile, M. Pelucchi, A. Frassoldati, A. Cuoci, T. Faravelli, E. Ranzi. *Biomass Bioenergy* **93**, 60 (2016).
[35] M. M. Mateus, N. F. Acero, J. C. Bordado, R. G. dos Santos. *Ind. Crops Prod.* **74**, 9 (2015).
[36] M. M. Mateus, D. Guerreiro, O. Ferreira, J. C. Bordado, R. dos Santos. *Cellulose* **24**, 659 (2017).
[37] L. P. Quoc, L. T. Giang, N. T. Hanh, G. T. Quyen, N. T. Thao. *J. Microbiol. Biotechnol. Food Sci.* **3**, 195 (2014).
[38] H. Brunnkvist, B. Karlberg, L. Gunnarsson, I. Granelli. *J. Chromatogr. B* **813**, 67 (2004).
[39] A. Tilmatine, M. Brahami, F. Miloua, R. Gouri, L. Dascalescu. *Front. Electr. Electron. Eng. China* **3**, 218 (2008).
[40] R. Jafari, B. E. Sundström, P. Holm. *Microb. Cell Fact.* **10**, 1 (2011).
[41] J. Xie, X. Zhai, C. Hse, T. Shupe, H. Pan. *Materials* **8**, 5472 (2015).
[42] M. Grilc, G. Veryasov, B. Likozar, A. Jesih, J. Levec. *Appl. Catal. B Environ.* **163**, 467 (2015).
[43] M. Grilc, B. Likozar, J. Levec. *Biomass Bioenergy* **63**, 300 (2014).
[44] B. Xiao, X. F. Sun, R. Sun. *Polym. Degrad. Stab.* **74**, 307 (2001).
[45] A. Synytsya, M. Novak. *Ann. Transl. Med.* **2**, 17 (2014).
[46] J. X. Sun, F. C. Mao, X. F. Sun, R. Sun. *J. Wood Chem. Technol.* **24**, 239 (2005).
[47] H. M. Liu, M. F. Li, S. Yang, R. C. Sun. *Energies* **6**, 1590 (2013).
[48] R. G. Dos Santos, R. Carvalho, E. R. Silva, J. C. Bordado, A. C. Cardoso, M. Do Rosário Costa, M. M. Mateus. *Ind. Crops Prod.* **84**, 314 (2016).
[49] M. Vale, M. M. Mateus, R. Galhano dos Santos, C. Nieto de Castro, A. de Schrijver, J. C. Bordado, A. C. Marques. *J. Clean. Prod.* **212**, 1036 (2019).
[50] R. Galhano dos Santos, N. F. Acero, S. Matos, R. Carvalho, M. Vale, A. C. Marques, J. C. Bordado, M. M. Mateus. *J. Polym. Environ.* **26**, 91 (2018).
[51] A. Barros-Timmons, N. V. Gama, R. Silva, C. P. Neto, A. Ferreira. *Adv. Mater. World Cong.* **62**, 13 (2017).
[52] M. M. Mateus, M. do Vale, A. Rodrigues, J. C. Bordado, R. Galhano dos Santos. *Energy* **124**, 40 (2017).
[53] L. A. Rosendahl (Ed.). *Direct Thermochemical Liquefaction for Energy Applications*. Woodhead Publishing, Sawston, Cambridge, UK (2018).